

Numerical Study of Solid Particles-Based Airlift Pump Performance

A-F. MAHROUS

Mechanical Power Engineering Department

Menoufiya University

Gamal Abdel-Nasser St., Shebin El-Kom, 32511

EGYPT

afmahrous@hotmail.co.uk

Abstract: - This work aims to numerically investigate the performance of airlift pump, lifting solid particles, under a variety of conditions. A numerical model of airlift pump based on the concept of momentum balance was developed and validated against available experimental data. Parametric predictive studies of the effects of solid particles conditions on model airlift pump performance were carried out. The predicted results showed that the solid particles volumetric concentration in the suction section of the airlift tube would significantly affect the airlift pump efficiency based on solids as the main gain of the pump. On the other hand, larger diameters of solid particles and higher input airflow rates would have a negative effect on the pump performance.

Key-Words: - Airlift pump, Performance study, Two-phase flow, Three-phase flow

1 Introduction

Airlift pumps provide a relatively simple and reliable method for difficult pumping applications. In the airlift system, air is injected at or near the base of a vertical pipe (the riser) that is partially submerged in a liquid (or liquid-solid mixture) through some injection system. Bubbles, therefore, form and expand as they rise. A two- (or three-) phase column containing air has a lower density than a column of liquid alone and consequently the mixture formed in the air-lift tube rises and is expelled at the top of the pump. Because of its simple construction and low maintenance requirements, airlift pump may be considered ideal for handling hazardous fluids in chemical and nuclear industries [1]. Airlift systems are also used as liquid-gas mixing devices in some of the most important chemical processes like hydrogenation and fermentation [2].

Numerous theoretical as well as experimental studies have been published related to the interpretation and analysis of airlift pump performance. Most of these studies have been concerned with the investigation into the influence of geometrical parameters and operational parameters on the performance of airlift pumps. Nicklin [3] proposed the first relatively useful theoretical treatment of flow through airlift pump based on momentum balance. Stenning and Martin [4] conducted an analytical and experimental

analysis of airlift pump taking into account the effects of fluid friction and slip between the air and liquid phases on the airlift pump performance. The operating performance predicted by such an analysis was predicted at the mean pump pressure which ceases to be valid for long airlift pumps. Boës et al. [5] proposed a theoretical model to predict the operation performance of airlift pump. In their analysis, they treated the two-phase water-solid mixture and the three-phase air-water-solid mixture as a homogenous mixture having mean density and mean velocity. Although the developed theoretical model did take into account the variation of air pressure and density throughout the lifting pipe, it was inadequate to a large extent. Clark et al. [6] published a comprehensive theoretical study on the airlift pump used for hydraulic transport of solids. They regarded the three-phase flow as a two-phase air-slurry flow. An equation for the design purpose of the airlift pump was developed based on the to-date literature on the two-phase flow theory. Yoshinaga and Sato [7] carried out an extensive experimental study to investigate the performance of airlift pump used for conveying uniform and non-uniform coarse particles. The experiments were examined with two airlift pumps having the same height but differ on tube diameter. Experiments were conducted using several combinations of ceramic balls with different volumetric flow rates. They also proposed a theoretical analysis to predict

the airlift pump performance based on the concept of momentum balance. A general calculation method for the three-phase air-liquid-solid flow and a design model for airlift pump installation were proposed by Margaritis and Papanikas [8]. The mathematical formulation was based on separated three-phase flow model. In their mathematical model, it was assumed that the liquid is the main phase and there were no interaction forces between air bubbles and solid particles. Hatta et al. [9] proposed a method for predicting the performance of airlift pump based on multi-fluid model. In the system of equations governing the air-liquid-solid three-phase flow field, the transitions of flow pattern of air-phase from bubbly to the churn flow has been taken into account. The phase interaction terms were introduced into the field equations.

The main objective of the present work was to numerically study the performance of airlift pump lifting solid particles under various geometrical and operational conditions. The numerical study was mainly based on the theoretical model proposed by [7]. The model has been validated against experimental measurements conducted on a model airlift pump.

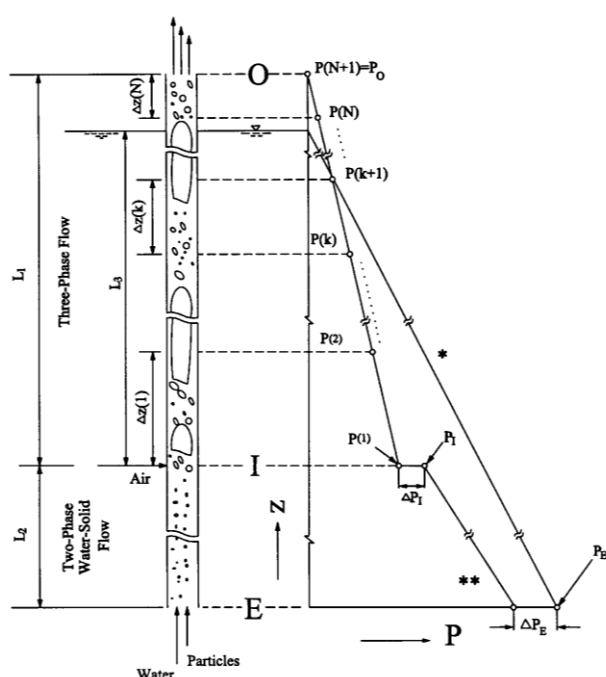


Fig. 1: Outline of the mixture flow and axial pressure distributions [7]. (*) Pressure distribution outside the pipe and (**) Pressure distribution inside the pipe.

2 Modeling Approach

2.1 Overview

In the present work, a numerical analysis of the performance of airlift pump based on the principle of momentum balance is presented under steady state operating conditions. The airlift pump performance is studied according to the analysis of [7]. The assumptions made for the mathematical formulation of the air-lift mechanism were: compressible and ideal gas flow for the air phase, the planes of equal velocity and equal pressure are normal to the pipe axis, no exchange of mass between phases, and isothermal flow for all phases. The assumption of isothermal flow is justified when the phases flow slowly through the airlift tube so that a continuous heat exchange with the environment is no longer possible, Margaritis and Papanikas [8].

The model to be studied theoretically here is shown in Fig. 1 together with a diagram of the pressure distribution, P , in the flow direction, z . The body of the airlift pump illustrated in Fig. 1 consists of two main parts. The first lower part is a suction pipe of length (L_2) between the bottom end and the air injection ports while the other part is a riser pipe of length (L_1) between the air and discharge ports. Throughout the suction pipe, the pressure gradient is larger than that due to hydrostatic pressure. That is owing to the weight of the solid-phase, when running with two-phase liquid-solid mixture, and pipe friction. On the other hand, the pressure gradient in the riser pipe is smaller than that of hydrostatic pressure. The reason is that the density of the two- or three-phase mixture is smaller than that of the pure liquid outside the pipe. The variation in mixture density predominates and it has a greater effect than that of the frictional pressure drop produced in the pipe. At the steady state condition, the airlift pumping system operates under these pressure distributions. The symbols E, I and O in Fig. 1 denote the cross sections of the suction pipe inlet, the air injector and the riser outlet, respectively. Generally, the solid particles to be conveyed are non-uniform in size and density and therefore it may be classified into "n" types according to their size and density. The solid-water mixture is sucked into the suction tube due to partial vacuum created by the injection of air into the injection ports.

2.2 Momentum Equation

The concept of momentum balance in the case of one-dimensional, steady and isothermal flow is applied to a control volume bounded by the pipe

wall and the cross sections E and O [7]. The momentum equation may therefore be written as:

$$\begin{aligned}
 & A \left[\rho_L j_L u_{L,E} + \sum_{i=1}^n \rho_S(i) j_S(i) u_{S,E}(i) \right] \\
 & - A \left[\rho_{G,O} j_{G,O} u_{G,O} + \rho_L j_L u_{L,O} + \sum_{i=1}^n \rho_S(i) j_S(i) u_{S,O}(i) \right] \\
 & - \pi D \int_E^O \tau_{LS} dz - \pi D \int_1^0 \tau_3 dz \\
 & - A \int_E^O \left[\rho_L \varepsilon_{L,LS} + \sum_{i=1}^n \rho_S(i) \varepsilon_{S,LS}(i) \right] g dz \\
 & - A \int_1^0 \left[\rho_G \varepsilon_G + \rho_L \varepsilon_{L,3} + \sum_{i=1}^n \rho_S(i) \varepsilon_{S,3}(i) \right] g dz \\
 & + A [\rho_L g (L_2 + L_3)] = 0
 \end{aligned} \tag{1}$$

Where ρ is the mass density, j is the average volumetric flux, A is the pipe cross-sectional area, u is the velocity, τ is the shear stress, ε is the volumetric fraction, g is the acceleration due to gravity, and i is the i^{th} rank of particles. The subscripts L, S and G denote the liquid, solid, and air-phases, respectively. Also, the subscripts LS and 3 represent the two-phase water-solid mixture and the three-phase air-water-solid mixture, respectively. In Equation 1, the first and second terms respectively denote the momentum which enters through E and leaves through O, the third and fourth terms denote the frictional forces in the suction and riser tubes, respectively, the fifth and sixth terms represent the weight of the two-phase water-solid mixture (in the suction pipe) and of the three-phase mixture (in the riser pipe), and the seventh term denotes the hydrostatic pressure force of the surrounding water, acting on the bottom end of the pipe at section E. Interaction forces between different phases, such as the drag and virtual mass forces, appear in the mathematical formulation only if the conservation equations of mass and momentum are applied for each phase separately.

Since both the air pressure and airflow rate vary throughout the pump owing to the expansion of air, the frictional and body forces in the riser tube section cannot be estimated at the mid section and, therefore, the riser tube should be divided into a number (N) of short segments in the flow direction. The length of each segment is chosen such that the nodes pressure ratio for any segment is the same for all segments. Assuming that the pressure distribution for each segment is linear, the frictional pressure gradient at such a segment and the flow local conditions are calculated at the middle of this segment. The terms of frictional and body forces in the momentum equation are then calculated using step-by-step integration procedure throughout the riser tube.

An iterative solution is required for the calculation of components flow rates and also for the other flow parameters that involved in the momentum equation. During the calculations, the air temperature at the injection point is assumed to be the same as the temperature of the water. Moreover, the temperature gradient is neglected through the riser tube. Therefore, an isothermal expansion of gas from the air injection pressure to the pump outlet pressure is applied. Performing the momentum balance over the entire length of the airlift tube, the airflow rate ($j_{G,O}$) aimed to achieve a specific gain of solid output rate can be numerically predicted. The numerical computations are also necessary for calculating the variations in air and water conditions throughout the individual sections of the airlift tube. Detailed information about the definition of different terms of Equation 1 can be found in the analysis of Yoshinaga and Sato [7] and in the research work of Mahrous [10].

2.3 Airlift Pump Efficiency

The most common engineering parameter that characterizes airlift pump performance is the airlift pump efficiency. Theoretical airlift pump efficiency (η_{th}) is simply defined as the ratio between the power required to lift the solid particles (or the liquid-phase) to the point of discharge and the power required to compress the air isothermally through the air compressor from the atmospheric pressure (P_0) to the air injection pressure (P_1). The power consumed due to isothermal compression of air is defined as:

$$N_C = P_0 A j_{G,O} \ln(P_1/P_0) \tag{2}$$

On the other hand, the net power gained is defined as the increase in the potential energy of liquid- or solid-phase depending on the gain of the pump. Considering the two cases and taking into account the Archimedes' principle for the case of lifting solids, the power gained is then given by:

$$\begin{aligned}
 N_G = C & \left[g(L_1 + L_2) A \sum_{i=1}^n \rho_S(i) j_S(i) - \rho_L g(L_2 + L_3) A \sum_{i=1}^n j_S(i) \right] \\
 & + (1-C) [\rho_L A j_L g(L_1 - L_3)]
 \end{aligned} \tag{3}$$

with $C = 0$ when lifting liquids or $C = 1$ while pumping solids is the main goal of the pump. Unless otherwise mentioned the definition of airlift pump efficiency presented in the subject of this work is based on the solids as the main gain of the pump, i.e. $C = 1$.

In view of that, the theoretical lifting efficiency is calculated according to the following equation:

$$\eta_{th} = \frac{N_G}{N_C} \quad (4)$$

In order to account for slip between the particles and the phases throughout the lifting pipe, an additional efficiency term called slip efficiency (η_s) is concerned. Concerning the N segments of riser tube, air injection section, outlet section, and the two-phase flow section, the slip efficiency (η_s) can be defined as [5]:

$$\begin{aligned} \eta_s &= \frac{1}{N+3} \sum \frac{\text{slip velocity}}{\text{mean flow velocity}} \\ &= 1 - \frac{1}{N+3} \sum \frac{U_{sw}}{j_G + j_L + \sum_{i=1}^n j_s(i)} \end{aligned} \quad (5)$$

where U_{sw} is the mean wall-affected free settling velocity of the particles and is defined as:

$$U_{sw} = \frac{1}{n} \sum_{i=1}^n u_{sw}(i) \quad (6)$$

The wall-affected free settling velocity of the solids of rank "i" is defined from:

$$u_{sw}(i) = \left[1 - \left\{ \frac{d_s(i)}{D} \right\}^2 \right] \left\{ 1 - \frac{\sum_{i=1}^n \varepsilon_{s,3}(i)}{1 - \varepsilon_G} \right\}^{2.4} \sqrt{\frac{\rho_L S(i) - 1}{\rho_A S(i) - 1}} u_{ST}(i) \quad (7)$$

where ρ_A is the apparent density of the mixture and S is the specific gravity of the solid particles and u_{ST} is the free settling velocity of a single solid particle in still water and is given by:

$$u_{ST}(i) = \sqrt{\frac{4}{3} \frac{g d_s(i)}{c_d(i)} \frac{(\rho_s(i) - \rho_L)}{\rho_L} f(i)} \quad (8)$$

where f and c_d are the form factor and drag coefficient of the particle.

If the loss of energy in the air compressor, including air conduit losses, is considered in an efficiency term called compressor efficiency (η_c), therefore the airlift pump overall efficiency is defined as:

$$\eta = \eta_{th} \eta_s \eta_c \quad (9)$$

3 Results and Discussion

3.1 Model Validation

In an attempt to verify the validity of the present theoretical treatment, the predicted airlift pump performance has been compared against experimental data measured by Weber and Dedegil [11] and with the data measured by Yoshinaga *et al.* [7, 12]. The experimental data together with their theoretical counterparts are plotted through

Fig. 2 to Fig. 4 to show the comparisons. The results show a typical example of the water pumped rate (j_L) as a function of air-supplying rate calculated at the standard atmospheric conditions ($j_{Ga} = Q_{G,O} / A$). Best fit for most of measured data points was obtained using pipe entry loss coefficient of 1.5. It has to be elucidated that De Cachard and Delhaye [13] proposed a value of the entry loss coefficient of about 3.4, as opposed to the value of 0.5 extensively used in the literature. The theoretical and experimental performance of airlift pump while lifting pure water have been compared through

Fig. 2 and Fig. 3 at different values of submergence ratio. The predicted performance displays the same general trend as the measured one Fig. 4 illustrates the variation of water volumetric flux while lifting a mixture of water and solid particles, against the volumetric flux of air. As illustrated in Fig. 2 to Fig. 4, the performance of airlift pump is well predicted by the developed numerical code over the entire range of presented submergence ratios. The comparison between the numerical and measured data, thus, demonstrates a high degree of agreement that is sufficient to justify the use of this simulation tool for parametric predictive studies.

In the following subsections, results of the effect of varying operation parameters on the airlift pump performance are predicted for the cases of lifting uniform and non-uniform solid particles. The predicted results are expressed by the variation of airlift pump efficiency against the airlift tube diameter. The common numerical conditions that have been assigned to the computer code are summarized in

Table 1. Unless otherwise mentioned, these values have been kept unchanged during different numerical runs. Numerically, the pump was used to lift solid particles at a constant volume flow rate of 80 cm³/sec through a lifting height of 2.4m and under 70% of submergence ratio.

Table 1: Numerical conditions

L_1	2 m	μ_G	11.9×10^{-6} Pa.sec
L_2	0.4 m	g	9.81 m/sec ²
α	0.7	ρ_S	2600 kg/m ³
P_O	1.013 bars	d_S	1 mm
T	293 K	Q_S	80 cm ³ /sec
R	287 J/kg K	c_d	0.42
ρ_L	1000 kg/m ³	f	1 (i.e. spherical particles)
v_L	10^{-6} m ² /sec	η_c	60 %

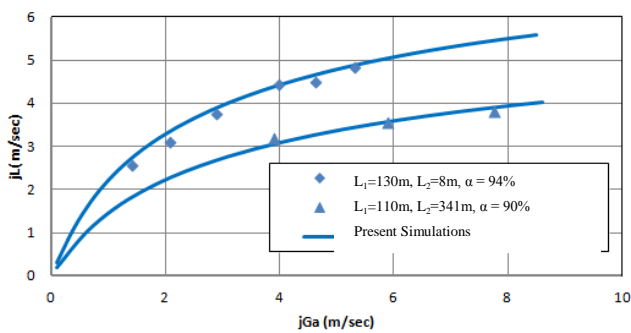


Fig. 2: Comparison of numerical results calculated based on present theoretical model with experimental data by Weber and Dedegil [11], $D=300mm$.

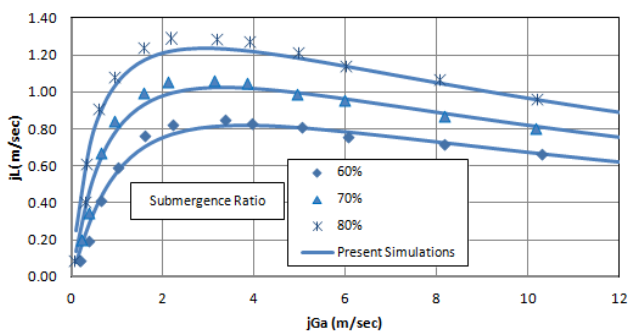


Fig. 3: Comparison of numerical results calculated based on present theoretical model with experimental data by Yoshinaga et al.[7, 12]. $D=26$ mm, $L_1=6.74m$ and $L_2=1.12m$.

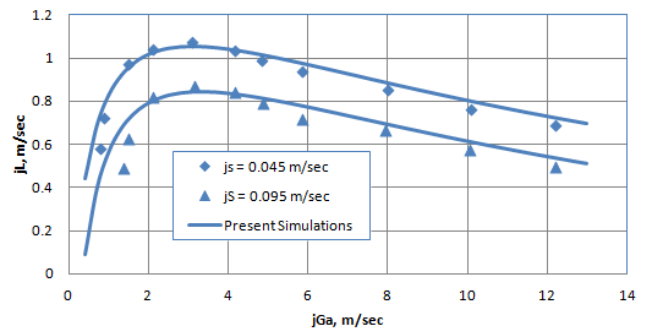


Fig. 4: Comparison of numerical results calculated based on present theoretical model with experimental data by Yoshinaga et al. [7, 12]. $D=26$ mm, $L_1=6.74m$ and $L_2=1.12m$, $\alpha = 0.8$, $d_s=6.12mm$, $\rho_s=2540kg/m^3$.

3.2 Performance of Airlift Pump Lifting Uniform Solid Particles

3.2.1 Effect of Pipe Diameter

The fundamental lifting characteristics of airlift pump with constant data are shown in Fig. 5. Airlift pump efficiency, input power, air injection pressure to atmospheric pressure ratio, and air to liquid volumetric flow ratio are plotted against the pipe diameter. The volumetric concentration of the discharged solid particles in the suction tube is defined as $\beta_s = j_s / (j_L + j_s)$. This concentration was kept constant at 16%. At smaller pipe diameters, the mean flow velocity increases and consequently the total pressure loss in the whole lifting pipe. The frictional power loss, as a result, significantly increases causing a decreasing in airlift pump efficiency. Any slight increase in the pipe diameter causes a considerable reduction in power loss and accordingly an increase in the pump efficiency is attained. At a certain value of pipe diameter the pump efficiency reaches a maximum value, for which the total pressure loss goes to minimum and hence the total power loss. Any further increase in the pipe diameter beyond the optimum value causes a drop in the efficiency curve. This could be attributed to the flow transition to annular flow regime [14, 15]. Practically, the optimum design of the airlift system should aim not only achieving the maximum efficiency but also a high enough efficiency for a wide range of operating conditions.

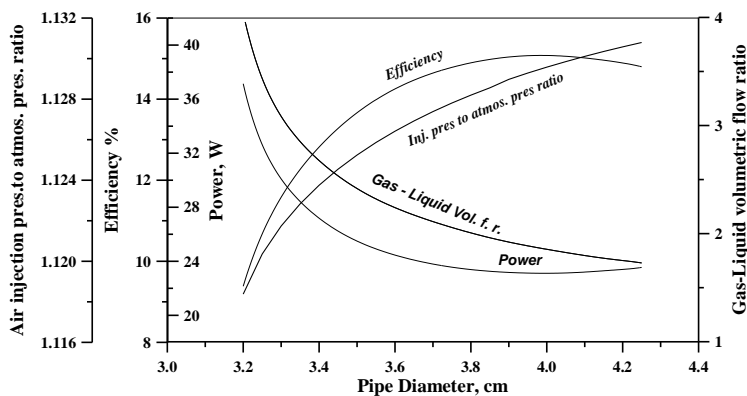


Fig. 5: Effect of pipe diameter on the performance of airlift pump operates at $\beta_s = 16 \%$.

As regards to the performance curve that shows the air injection pressure to atmospheric pressure ratio with respect to pipe diameter, as the pipe diameter increases, the air injection pressure to atmospheric pressure ratio is increasing as well. This behavior is logically understood from the simple Bernoulli's equation for a single-phase having a constant density. That equation, when applied in the two-phase flow section, indicates that as the pipe diameter increases, and hence a reduction in the flow velocity takes place, the various head losses will be decreasing. Thus, the downstream mixture pressure would be increasing, since the upstream pressure does not change.

3.2.2 Effect of Solid Particles Volumetric Concentration

Fig. 6 shows the effect of solid particles concentration (β_s) on the performance of airlift pump. As can be seen, as the concentration of solid particles in the suction tube increases, the airlift pump efficiency also increases. So, in order to operate the system safely and more efficiently, it should be operated with large solid particle concentration but without blocking the lifting pipe. As illustrated in Fig. 6, optimum efficiency takes place at smaller tube diameters when increasing the degree of solids concentration in the suction tube.

3.2.3 Effect of Solid Particles Diameter

For a single rank of particles, the qualitative influence of solid particles diameter on the lifting characteristics of airlift pump is displayed in Fig. 7. It is clear that the pump efficiency depends greatly on the solid particle diameter. At a constant value of pipe diameter, as the solid particles diameter increases, the airlift pump efficiency decreases. The reason for such behavior is that by increasing the diameter of solid particles, keeping Q_s constant, the

free settling velocity is accordingly increased (Equation 7). This yields to an increase in the slip between the particles and the mean flow. Besides, the force needed to lift solids is much greater for particles with larger size than that with smaller one. The two factors considered above are responsible for the reduction in the airlift pump efficiency owing to increasing the particles diameter.

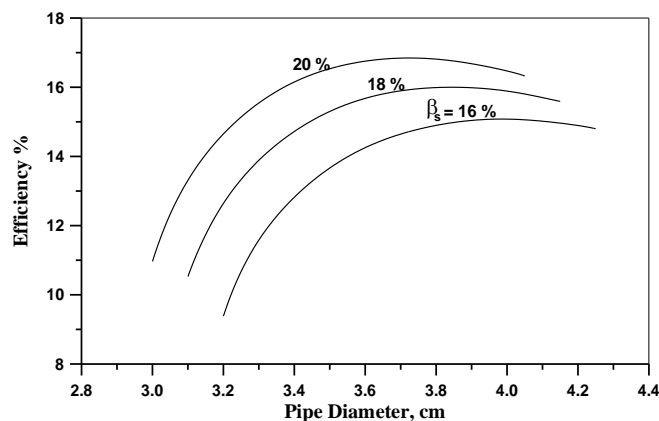


Fig. 6: Effect of solid particles volumetric concentration (β_s) on airlift pump performance.

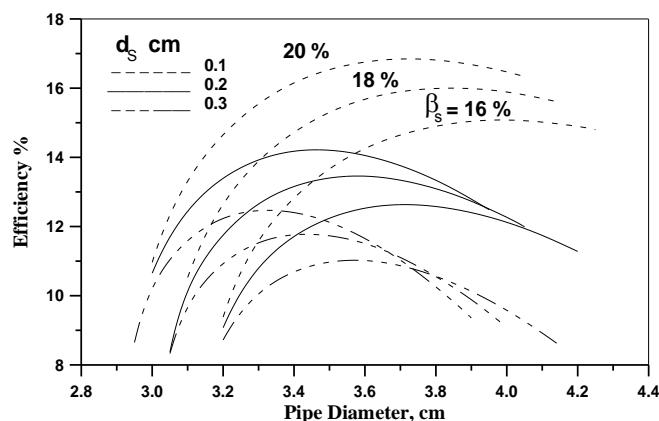


Fig. 7: Effect of solid particles diameter on airlift pump performance.

3.2.4 Effect of Solid Particles Density

The effect of solid particles density on the performance of airlift pump is illustrated in Fig. 8. It can be clearly seen from this Fig. that, as the solid particles density increases, under otherwise constant conditions, the airlift pump optimum efficiency also increases. The settling velocity of solid particles, Equation 7, increases with the increase in particles density. For particles with higher settling velocity, greater water velocities are required to initiate

lifting of solids and thus higher volumetric airflow rates are demanded. The drop in the total pressure owing to the weight of the mixture increases at higher settling velocities whereas the solid particles cause higher volumetric concentration, higher solid-liquid mixture density (ρ_{LS}), and higher pressure gradients due to their lower absolute velocity. Increasing the total pressure loss in the two-phase flow section has the tendency to decrease the air pressure at the injection zone. Moreover, according to the definition of Equation 3, it is noticed that, by increasing the solid particles density, the power required to lift the dense phase (N_G) also increases. Increasing the useful power and decreasing the air injection pressure, by increasing the solid particles density, lead to an increase in the airlift pump theoretical efficiency.

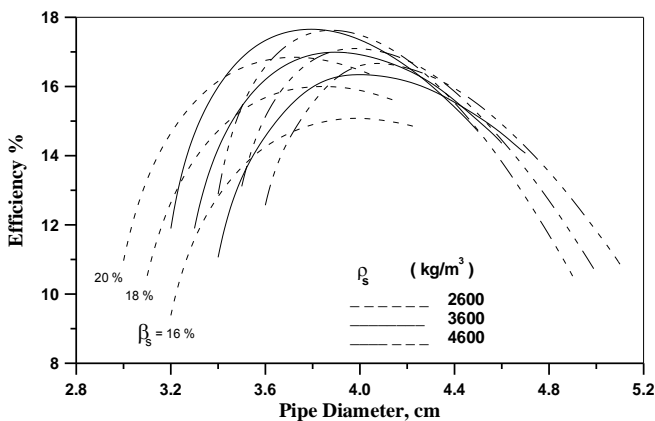


Fig. 8: Effect of solid particles density on airlift pump performance.

3.2.5 Effect of Solids Flow Rate

The performance of airlift pump is numerically examined for three values of solid particles volumetric flow rate, namely 60, 80 and 100 cm^3/sec . The qualitative dependence of the conveying characteristics on Q_s is shown in Fig. 9. It is noticed that for the three displayed sets of plots, the family of curves corresponding to a certain volumetric flow rate of solid particles is fairly similar to those obtained at other values but shifted in the direction of pipe diameter. As the volumetric flow of solid phase increases, the mean flow velocity increases as well. The increase in the mean flow velocity causes a corresponding increase in the head losses and as a result the efficiency of the airlift pump decreases. In order to keep the pump efficiency as constant as possible, in such a case, the

head losses should be decreased and this could be attained by increasing the pipe diameter.

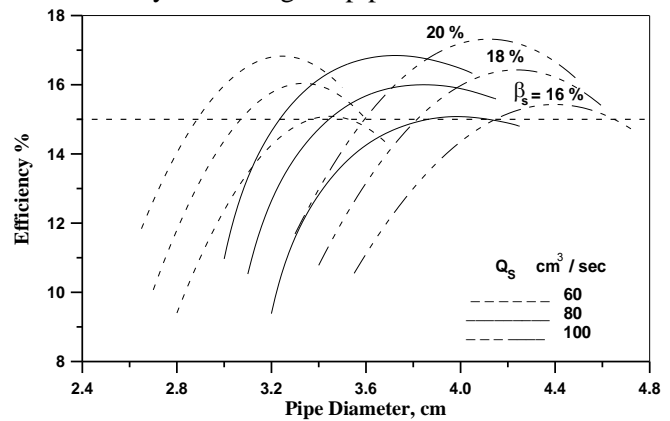


Fig. 9: Effect of solid particles flow rate on airlift pump performance.

3.2.6 Effect of Solid Particles Form Factor

Fig. 10 presents the theoretical characteristics of airlift pump used to lift coarse particles having three values of form factor, namely 0.5, 0.75 and 1. It is commonly accepted that the drag coefficient of the solids depends on particles Reynolds number and their shape factor. In the present subsection, the effect of solid particles form factor on the airlift pump performance is solely considered. The numerical results of Fig. 10 show that, as the form factor of solid particles decreases, at a certain value of pipe diameter, the pump efficiency is increased.

3.2.7 Effect of Solid Particles Drag Coefficient

As illustrated in Fig. 11, by increasing the drag coefficient of solid particles, the airlift pump efficiency is also increasing. Increasing the drag coefficient of solid particles means increasing the viscous force, while keeping the mean flow velocity unaffected. This would result in an increase in the total pressure loss in the two-phase flow section and consequently decreases the air injection pressure. Furthermore, as the viscous force increases owing to drag coefficient, the amount of lifted liquid decreases and therefore the air to liquid volumetric flow ratio increases, for the same conditions of the injected air. The combined effect of the increased air to liquid volumetric flow ratio and the decreased air pressure at the injection zone improves the airlift pump efficiency.

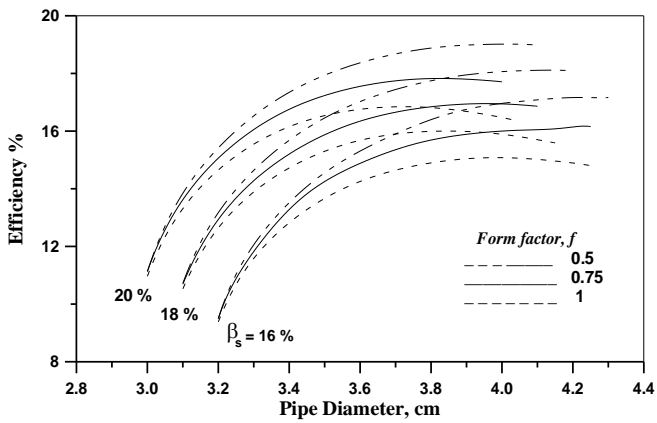


Fig. 10: Effect of solid particles form factor on airlift pump performance.

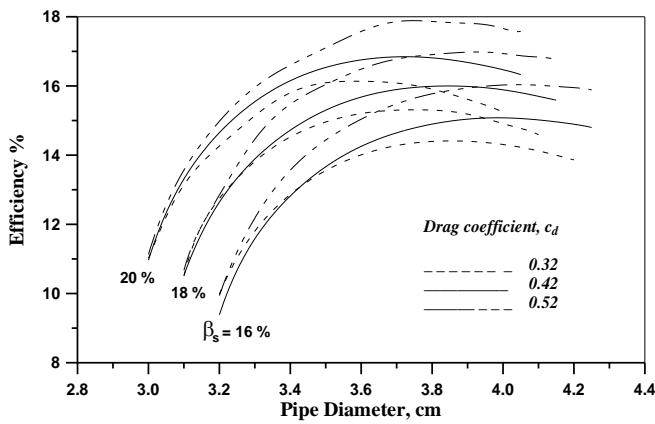


Fig. 11: Effect of drag coefficient of solid particles on airlift pump performance.

3.3 Performance of Airlift Pump Lifting Non-Uniform Solid Particles

The following subsections are concerned with the predicted performance of airlift pump used for lifting two ranks of particles, mixed together; differ either in density or in size.

3.3.1 Effect of Combining Two Ranks of Particles at Different Weights

Fig. 12 shows the effect of combining two types of particles; differ only in density, at different mixing ratio. The mixing ratio (M_s^*) is defined according to the following equation:

$$M_s^* = \frac{\dot{m}_{s1}}{\dot{m}_s} \tag{10}$$

Here \dot{m}_{s1} is the mass flow rate of solid particles of relative density 2.6 and \dot{m}_s is the total mass flow rate of solid particles.

Trial calculations have therefore been done for three values of M_s^* , namely 0.4, 0.6, and 1. It is apparent that, by decreasing the mixing ratio, the total solid particles mass flow rate increases. This effect tends to increase the total head loss in the suction tube as well as in the riser tube, and accordingly the useful power required to lift the dense phase would also be increasing. This yields to an increase in the airlift pump efficiency.

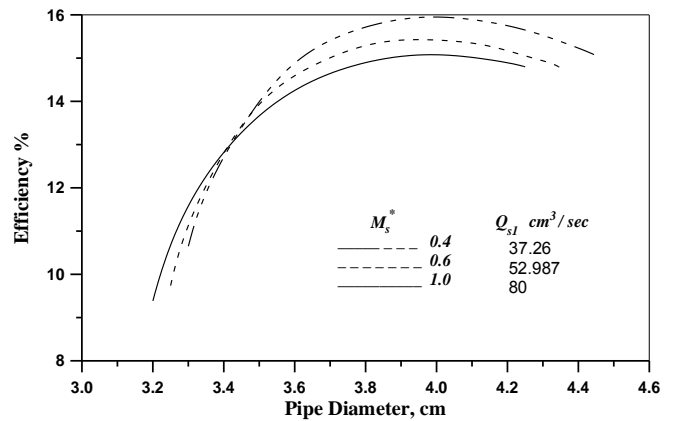


Fig. 12: Effect of combining two ranks of particles at different weights. $d_{s1} = d_{s2} = 1 \text{ mm}$, $\rho_{s1} = 2600 \text{ kg/m}^3$, $\rho_{s2} = 3400 \text{ kg/m}^3$, $Q_s = 80 \text{ cm}^3/\text{sec}$ and $\beta_s = 16 \%$.

3.3.2 Effect of Combining Two Ranks of Particles at Different Diameters

The effect of combine two ranks of solid particles at different diameters on the airlift pump performance is shown in

Fig. 13. The results may be interpreted in a very similar way to that in Section 0, the effect of solid particles diameter on the performance of airlift pump. However, combining two ranks of particles differ only in diameters has a minor negative influence on the general lifting performance than that obtained due to increasing the particles diameter.

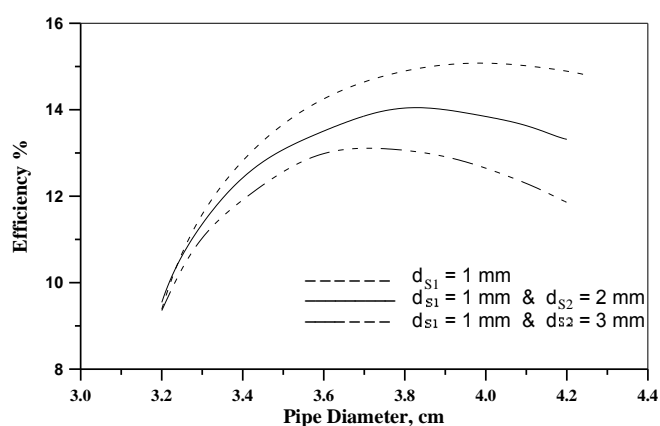


Fig. 13: Effect of combining two ranks of particles at different diameters. $\rho_{S1} = \rho_{S2} = 2600 \text{ kg/m}^3$, $Q_{S1} = Q_{S2} = 40 \text{ cm}^3/\text{sec}$, and $\beta_s = 16 \%$.

4 Conclusions

The performance of airlift pump depends on two sets of parameters; the geometrical and operational parameters. A numerical investigation into the impact of solid particles operational parameters on airlift pump lifting characteristics has numerically been conducted. The numerical model has been validated against available experimental data and the comparison has demonstrated a degree of agreement sufficient to justify the use of this simulation tool for parametric predictive studies. The predicted results showed that larger diameters of solid particles would have a negative effect on the airlift pump performance, due to the increase in the power required for the pumping action. On the other hand, the pump volumetric concentration of solid particles in the suction pipe has shown positive effects on the pump performance. The other parameters, like form factor and drag coefficient of the lifted solid phase, have slight effects on the airlift pump performance. The objective of airlift designers is to combine the effects of geometrical and operational parameters in order to optimize the airlift pump performance as well as to maintain a satisfactory operation over a wide range of conditions.

List of Symbols

- A Pipe cross sectional area (m^2).
- D Pipe diameter (m).
- d_s Diameter of solid particles (m).
- C Constant.

- c_d Drag coefficient.
- g Acceleration due to gravity (m/sec^2).
- f Form factor of solid particles
- i Index denotes the type of solid phase.
- j Average volumetric flux (m/sec).
- k Index.
- L_1 Riser tube length (m).
- L_2 Suction tube length (m).
- L_3 Submergence height (m).
- N Number of riser tube segments.
- N Power (Watts).
- n Number of types of solid particles.
- P Pressure (Pa).
- Q_s Volumetric flow rate of solids (cm^3/sec).
- R Universal gas constant (J/kg.K).
- S Specific gravity.
- u Velocity (m/sec).
- z Elevation of the mixture level in the pipe (m).

Greek symbols:

- α Submergence ratio (L_3 / L_1).
- β_s Volumetric concentration of solids in suction tube
- ε Volumetric fraction.
- ρ Density (kg/m^3).
- η Efficiency
- τ Shear stress (N/m^2).
- ν Kinematic viscosity (m^2/sec)

Subscripts:

- 2 Two-phase water-solid mixture.
- 3 Three-phase air-water-solid mixture
- a Atmospheric conditions.
- C Consumed.
- E Pipe inlet section.
- G Gas phase.
- G Gained
- I Injection.
- L Liquid phase.
- LS Two-phase liquid-solid
- O Pipe outlet section.
- S Solid phase
- th Theoretical.

References:

1. Clark, N.N., *Pumping Toxic and Radioactive Fluids with Air Lifts*, in *United States Environmental Protection Agency, Office of Research and Development, EPA 600/9-85/025*. 1985. p. 426-432.

2. Dedegil, M.Y., *Principles of airlift techniques*, in *Encyclopedia of Fluid Mechanics*, N.P. Chereimisinoff, Editor. 1986, Gulf, Houston, TX. p. Chapter 12.
3. Nicklin, D.J., *The Airlift Pump: Theory and Optimization*. Trans. Instn Chem. Engrs, 1963. **41**: p. 29-39.
4. Stenning, A.H. and C.B. Martin, *An Analytical and Experimental Study of Airlift Pump Performance*. Journal of Engineering for Power, Trans. of the ASME, Series A, 1968. **90**(2): p. 106-110.
5. Boës, C., Düring, R. and Wasserroth, E., *Airlift as a drive for single and double pipe conveying plants (Airlift als antrieb für einrohr-und doppelrohr-förderanlagen)*. fördern und heben, 1972. **22**(7): p. 367-378 (In German).
6. Clark, N.N., Flemmer, R.L.C., and Meloy, T.P., *Air Lift Pumps for Hydraulic Transport of Solids*, in *9th Annual Powder and Bulk Solids Conf.* 1984: Rosemont, Illinois. p. 446-456.
7. Yoshinaga, T. and Y. Sato, *Performance of an air-lift pump for conveying coarse particles*. Int. J. Multiphase Flow, 1996. **22**(2): p. 223-238.
8. Margaris, D.P. and D.G. Papanikas, *A generalized gas-liquid-solid three-phase flow analysis for airlift pump design*. Trans. of the ASME, J. of Fluids Engineering, 1997. **119**: p. 995-1002.
9. Hatta, N., Fujimoto, H., Isobe, M. and Kang, J., *Theoretical analysis of flow characteristics of multiphase mixtures in a vertical Pipe*. Int. J. Multiphase Flow, 1998. **24**(4): p. 539-561.
10. Mahrous, A.-F., *Performance of airlift pumps*, in *Mechanical Power Engineering Dept.* 2001, Menoufiya University, Egypt.
11. Weber, M. and Y. Dedegil, *Transport of solids according to the air-lift principle*, in *Proc. 4th International Conf. on the Hydraulic Transport of Solids in Pipes*. 1976. p. H1-1 - H1-23.
12. Yoshinaga, T., Sato, Y. and Sadatomi, M., *Characteristics of air-lift pump for conveying solid particles*. Jap. J. Multiphase Flow, 1990. **4**: p. 174-191 (in Japanese).
13. De Cachard, F. and J.M. Delhaye, *A Slug-Churn Flow Model for Small-Diameter Airlift Pumps*. Int. J. Multiphase Flow, 1996. **22**(4): p. 627-649.
14. Kassab, S.Z., Kandil, H.A., Warda, H.A. and Ahmed, W.H., *Air-lift pumps characteristics under two-phase flow conditions*. Int. J. Heat and Fluid Flow, 2009. **30**: p. 88-98.
15. Samaras, V.C. and D.P. Margaris, *Two-phase flow regime maps for air-lift pump vertical upward gas-liquid flow*. Int. J. Multiphase Flow, 2005. **31**: p. 757-766.